3′-Azido-3′-deoxythymidine-(5′)-tetraphospho-(5′)-adenosine, the Product of ATP-Mediated Excision of Chain-Terminating AZTMP, Is a Potent Chain-Terminating Substrate for HIV-1 Reverse Transcriptase†

Sanjeewa Dharmasena,‡ Zita Pongracz,‡ Eddy Arnold,§ Stefan G. Sarafianos,§,|| and Michael A. Parniak*,‡

Division of Infectious Diseases, Department of Medicine, University of Pittsburgh School of Medicine, Pittsburgh, Pennsylvania 15261, and Center for Advanced Biotechnology and Medicine and Department of Chemistry and Chemical Biology, Rutgers University, Piscataway, New Jersey 08854

Received July 6, 2006; Revised Manuscript Received October 26, 2006

ABSTRACT: The resistance of HIV-1 to 3′-azido-3′-deoxythymidine (AZT) involves phosphorolytic excision of chain-terminating AZT-5′-monophosphate (AZTMP). Both pyrophosphate (PP_i) and ATP act as excision substrates in vitro, but the intracellular substrate used during replication of AZT-resistant HIV is still unknown. PP_i-mediated excision produces AZT-5′-triphosphate (AZTTP), which could be immediately re-used as a substrate for viral DNA chain termination. In contrast, ATP-mediated excision produces the novel compound AZT-(5′)-tetraphospho-(5′)-adenosine (AZTp4A). Since little is known of the interaction of AZTp4A with HIV-1 RT, we carried out kinetic and molecular modeling studies to probe this. AZTp4A was found to be a potent inhibitor of HIV-1 RT-catalyzed DNA synthesis and of both ATP- and PP_i-mediated AZTMP excision. AZTp4A is in fact an excellent chain-terminating substrate for AZT-resistant RT-catalyzed DNA synthesis, better than AZTTP (k_{pol}/K_d = 6.2 and 11.9 for AZTTP and AZTp4A, respectively). The affinity of AZT-resistant HIV-1 RT for AZTp4A is at least 30000-fold greater than that for the excision substrate ATP and ∼10-fold greater than that for AZTTP. Dissociation of newly formed AZTp4A from RT may therefore provide a significant rate-limiting step for continued HIV-1 DNA synthesis. Our studies show that the products of PP_i- and ATP-mediated excision of chain-terminating AZTMP (AZTTP and AZTp4A, respectively) are both potent chain-terminating substrates for HIV-1 RT, suggesting that there is no obvious benefit to HIV using ATP instead of PP_i as the excision substrate.

Replication of the human immunodeficiency virus (HIV)[1] is absolutely dependent on the viral enzyme reverse transcriptase (RT), a DNA polymerase that catalyzes all steps in the conversion of HIV genomic RNA into double-stranded viral DNA that can be integrated into the host genome (*1*, *2*). Because of its essential nature in HIV replication, RT has been a widely studied target for antiretroviral drug discovery. Indeed, as of mid-2006, 11 of the current clinically used drugs for the treatment of HIV infection are inhibitors of HIV RT. Eight of the therapeutic RT inhibitors are nucleoside or nucleotide reverse transcriptase inhibitors (NRTIs), and these are among the most widely used in current clinical treatment of HIV infection.

Antiretroviral NRTIs are 2′-deoxyribonucleoside analogues that lack a 3′-OH group on the ribose moiety. After intracellular conversion to the active 5′-triphosphate form, NRTI-TP inhibits DNA synthesis by competing with the natural nucleotides both for recognition by RT as a substrate and by incorporation into the nascent viral DNA chain (*3*). Incorporation of an NRTI into the nascent viral DNA chain by RT results in termination of DNA synthesis. Unfortunately, the prevalence of drug-resistant HIV-1 variants limits the continued clinical efficacy of NRTIs (*4*). Two different mechanisms account for phenotypic resistance of HIV-1 to NRTIs (*5*, *6*). One is NRTI discrimination in which the mutant RT preferentially incorporates the natural dNTP rather than the homologous NRTI-TP. The other involves phosphorolytic excision of the incorporated chain-terminating NRTI from the 3′-end of the primer (*7*−*9*). The excision phenotype is primarily associated with mutations arising in resistance to AZT (*7*, *9*, *10*). These mutations, termed thymidine analogue mutations (TAMs), include M41L, D67N, K70R, T215F/Y, and K219Q among others (*11*−*14*).

A number of different acceptor substrates have been shown to function in the phosphorolytic excision phenotype in vitro, including pyrophosphate (PP_i) (*7*) and ATP (*8*, *9*). Indeed, virtually any ribonucleotide or deoxyribonucleotide diphos-

† This work was supported by National Institutes of Health Grants AI52010 and AI60452 (M.A.P.).

* To whom correspondence should be addressed: Department of Molecular Genetics and Biochemistry, University of Pittsburgh, BST W1142, 200 Lothrop St., Pittsburgh, PA 15261. Telephone: (412) 648-8884. Fax: (412) 648-9653. E-mail: parniak@mgb.pitt.edu.

‡ University of Pittsburgh School of Medicine.

§ Rutgers University.

|| Current address: Department of Molecular Microbiology and Immunology, University of Missouri School of Medicine, 401 Life Sciences Center, 1201 Rollins Dr., Columbia, MO 65211.

[1] Abbreviations: AZT, 3′-azido-3′-deoxythymidine; AZTMP, 3′-azido-3′-deoxythymidine-5′-monophosphate; AZTTP, 3′-azido-3′-deoxythymidine-5′-triphosphate; AZTp4A, 3′-azido-3′-deoxythymidine-(5′)-tetraphospho-(5′)-adenosine; HIV-1, human immunodeficiency virus type 1; PP_i, pyrophosphate; RT, reverse transcriptase; TAM-RT, reverse transcriptase containing the D67N, K70R, T215F, and K219Q mutations; T/P, template−primer; wt, wild type.

10.1021/bi061364s CCC: $37.00
Published on Web 12/21/2006

phate or triphosphate can serve as an acceptor in vitro (*8*). However, the concentrations needed for the excision reaction are generally well above the expected cellular levels of all acceptor substrates, except PP_i and ATP, suggesting that only the latter two compounds may be important in the in vivo resistance phenotype. Nonetheless, the identity of the substrate(s) used for the NRTI excision reaction during replication of AZT-resistant HIV is not yet known with certainty. There are benefits and drawbacks to ATP or PP_i as the excision substrate. RT-catalyzed excision of 3′-terminal AZTMP in vitro is readily demonstrable with putative physiological levels of PP_i (50−150 μM) or ATP (3 mM). The rate of AZTMP excision is substantially higher with PP_i than with ATP as the substrate, although differences in excision between wild-type and TAM-containing RT are generally more readily seen with ATP as the substrate. A major potential drawback for PP_i as an excision substrate is the fact that PP_i-mediated excision produces AZT-5′-triphosphate (AZTTP), which could be immediately re-used as a substrate for viral DNA chain termination. In contrast, ATP-mediated excision produces the novel compound 3′-azido-3′-deoxythymidine-(5′)-tetraphospho-(5′)-adenosine (AZTp4A). HIV RT has been shown to use certain dinucleoside 5′,5′-tetraphosphates as substrates although less efficiently than the corresponding deoxynucleoside triphosphates (*15*). However, virtually nothing is known about the interaction of AZTp4A with HIV RT.

In this work, we studied this interaction and found that AZTp4A is an excellent substrate for TAM-RT and that use of this compound as a substrate for HIV-1 RT results in a 3′-AZTMP-terminated primer. The affinity of TAM-RT for AZTp4A appears to be orders of magnitude higher than that for ATP and TTP. Our data suggest that release of newly formed AZTp4A is likely to be a crucial rate-limiting step for continued viral DNA synthesis catalyzed by TAM-RT. Furthermore, since the products of both PP_i- and ATP-mediated excision of chain-terminating AZTMP (AZTTP and AZTp4A, respectively) are both potent chain-terminating substrates for HIV-1 RT, there may be no obvious benefit to HIV using ATP instead of PP_i as the excision substrate.

EXPERIMENTAL PROCEDURES

Reagents. The wild type (wt) and TAM-RT with the D67N, K70R, T215F, and K219Q mutations were expressed and purified using methods previously described (*16*). We used the T215F mutation rather than T215Y, as the T215F mutation has been shown to be more closely associated with K70R and K219Q mutations in clinical isolates, whereas the T215Y mutation is more closely associated with the M41L and L210W mutations (*17*). The protein concentration of the purified enzymes was determined by spectrophotometry at 280 nm using an extinction coefficient of 260 450 M^{-1} cm^{-1}. The active site concentrations of RT were calculated from pre-steady-state burst experiments (*18*). Burst amplitudes of 69 and 66% were calculated for the wt and TAM-RT enzyme-purified preparations, respectively. All pre-steady-state kinetic experiments were performed using corrected RT active site concentrations. Unlabeled dNTPs were purchased from Promega (Madison, WI). [^{3}H]TTP and [γ-^{32}P]ATP were products of Perkin-Elmer Life Sciences (Boston, MA). The homopolymeric template−primers (T/P) poly(rA)-oligo-$(dT)_{12-18}$ and poly(rC)-oligo$(dG)_{12-18}$ used for steady-state kinetic studies were obtained from Amersham Biosciences (now GE Healthcare, Piscataway, NJ). AZTTP and AZTp4A (as a custom synthesis) as well as the 19-nucleotide DNA primer (3′-CAGGGGGGAAAAGAAAATT-5′) and the 57-nucleotide DNA template (5′-CGT TGT CAG TGA ATC AGC CCT TCC AGT CCC CCC TTT TCT TTT AAA AAG TGG CTA AGA-3′) oligonucleotides used to prepare the heteropolymeric T/P were obtained from Trilink Biotechnologies (San Diego, CA). We used only this single heteropolymeric template−primer pair in this study as sequence context effects on AZTTP incorporation and AZTMP excision appear to be minimal (*19*). All the other reagents were of the highest quality available and were used without further purification.

The 19-nucleotide DNA primer was 5′-radiolabeled with [γ-^{32}P]ATP and T4 polynucleotide kinase (New England BioLabs, Ipswich, MA) according to suppliers' instructions. The labeled primer was purified using denaturing polyacrylamide gel electrophoresis on 7 M urea−16% polyacrylamide gels followed by elution from the gel. The purified 5′-^{32}P-labeled primer was then annealed to the 57-nucleotide DNA template using a 1:1.2 molar ratio of template to primer by heating to 90 °C followed by slow cooling to ambient temperature to form the 57-nucleotide/19-nucleotide template−primer (57/19 T/P) substrate. The concentration of the T/P was verified by UV absorbance at 260 nm. Labeled T/P was stored at −20 °C until it was used.

Steady-State Analysis of RT DNA Polymerase Activity. In one experimental approach, wt and TAM-RT RNA-dependent DNA polymerase activity in the absence or presence of the inhibitor was determined using 0.2 unit/mL poly(rA)-oligo$(dT)_{12-18}$, 2 nM RT, and 5 μM [^{3}H]TTP in a final volume of 50 μL of 50 mM Tris-HCl (pH 8.0) containing 60 mM KCl and 10 mM $MgCl_2$. Samples were incubated for 20 min at 37 °C and then reactions quenched by adding 200 μL of ice-cold 10% trichloroacetic acid containing 20 mM sodium pyrophosphate. After incubation for 20 min on ice, samples were filtered through a 1.2 μm glass fiber type C filter in 96-well microplates (Millipore, Bedford, MA). The filters were washed sequentially with 10% TCA and ethanol, and the extent of incorporation of [^{3}H]TMP into the precipitated nucleic acid was quantified by liquid scintillation spectrometry.

The heteropolymeric 57/19 T/P described above was used for other experiments. Three different experimental conditions were used. In all, RT (40 nM) was incubated with T/P (150 nM) in 50 mM Tris-HCl (pH 8.0) containing 60 mM KCl, 10 mM $MgCl_2$, and 0.01 unit of inorganic pyrophosphatase for 5 min at 37 °C. In one approach, reactions were initiated by the addition of varying concentrations of AZTTP or AZTp4A only. In the second approach, reactions were initiated by the addition of varying concentrations of AZTTP or AZTp4A followed by incubation for 20 min at 37 °C. Then TTP, dATP, and dGTP (2 μM each) were added, and the reaction was allowed to proceed for an additional 20 min to allow extension of any non-chain-terminated primer. In the third approach, reactions were initiated by the addition of varying concentrations of AZTTP or AZTp4A with TTP, dATP, and dGTP (2 μM each) followed by incubation for 20 min at 37 °C. In all approaches, control reactions substituted TTP for AZTTP or AZTp4A. Reactions were terminated by the addition of an equal volume of gel loading

buffer [98% deionized formamide, 10 mM EDTA, and bromophenol blue and xylene cyanol (1 mg/mL each)], and mixutres were denatured by being heated at 85 °C for 5 min, followed by electrophoretic resolution of the products on a 7 M urea−16% polyacrylamide gel. The resolved products were quantified by phosphorimaging using a Bio-Rad GS525 Molecular Imager (Bio-Rad, Hercules, CA).

Pre-Steady-State Kinetic Experiments and Product Analysis. Pre-steady-state reactions on the time scale of 10 ms to 5 s were carried out using a Bio-Logic (Claix, France) SFM-400 instrument. Briefly, reactions were performed at 37 °C in 50 mM Tris-HCl (pH 8.0) containing 50 mM KCl, 10 mM $MgCl_2$, and varying concentrations of the nucleotide substrates. HIV-1 RT was preincubated with T/P prior to rapid mixing with nucleotide and divalent metal ions to initiate the reaction. All reported concentrations of RT are the final concentrations of RT active sites in the mixed reaction. The concentrations of T/P also refer to those after mixing. After varying times, the reactions were quenched with 0.5 M EDTA. Quenched samples were mixed with an equal volume of gel loading buffer and denatured, and the products were resolved by electrophoresis on a 7 M urea−16% polyacrylamide gel and quantified by phosphorimaging.

Both pre-steady-state burst and single-turnover experiments were performed in characterizing the kinetics of incorporation of TTP, AZTTP, and AZTp4A. Burst experiments used T/P concentrations 3 times greater than those of the RT active site concentration. Single-turnover experiments were used to determine K_D and k_{pol} and generally used RT in a 3−4-fold excess relative to the concentration of T/P.

Data Analysis. Kinetics data were analyzed by nonlinear regression using Sigma Plot (Systat Software, Point Richmond, CA). Data from burst reactions were analyzed using

$$[\text{20-nucleotide product}] = A[1 - \exp(-k_{obs}t) + k_{ss}t] \quad (1)$$

where A is the amplitude of the burst, which reflects the concentration of RT active sites, k_{obs} is the observed first-order rate constant for nucleotide substrate incorporation, and k_{ss} is the observed steady-state rate constant.

Single-turnover experimental data were analyzed using

$$[\text{20-nucleotide product}] = A[1 - \exp(-k_{obs}t)] \quad (2)$$

to determine the rate of nucleotide incorporation (k_{obs}) at any given nucleotide concentration. The dissociation constant K_d was determined by fitting the observed rate constants (k_{obs}) at different concentrations of nucleotide to the hyperbolic equation

$$k_{obs} = (k_{pol}[\text{dNTP}])/(K_d + [\text{dNTP}]) \quad (3)$$

where k_{pol} is the first-order rate constant for maximum nucleotide incorporation and K_d is the equilibrium dissociation constant for the interaction of nucleotides with the RT−T/P complex (*7*, *18*, *20*).

Assay of RT-Catalyzed Phosphorolysis. AZTMP was added to the primer 3′-terminus of the 57-nucleotide/5′-[^{32}P]-19-nucleotide T/P by incubation with wt RT and 100 μM AZTTP for 30 min at 37 °C. The resulting ^{32}P-labeled, chain-terminated 20-nucleotide primer was purified by elution of the appropriate band following electrophoretic resolution on 7 M urea−16% acrylamide denaturing gels. The purified chain-terminated primer was then reannealed to the 57-nucleotide DNA template−DNA primer and stored at −20 °C for use as T/P in phosphorolysis experiments.

Two types of phosphorolysis experiment were carried out. In the "direct" assay, the phosphorolytic removal of 3′-AZTMP in the absence or presence of varying concentrations of AZTp4A was assayed by incubating wt or TAM-RT with the AZTMP-terminated T/P (4:1 RT:T/P ratio) in 50 mM Tris-HCl (pH 8.0) and 50 mM KCl. Reactions were initiated by the addition of 10 mM $MgCl_2$ and 50−150 μM PP_i or 3.0 mM ATP. Inorganic pyrophosphatase (0.01 unit; Sigma) was included in phosphorolysis reactions using ATP, to ensure removal of any contaminating PP_i in the ATP preparation. Aliquots were removed at defined times and quenched with equal volumes of gel loading dye [98% deionized formamide, 10 mM EDTA, and bromophenol blue and xylene cyanol (1 mg/mL each)]. The 20-nucleotide 3′-AZTMP-terminated substrate and 19-nucleotide excision products were separated by denaturing gel electrophoresis and quantified by phosphorimaging.

RT-catalyzed phosphorolytic "rescue" DNA synthesis using AZTMP-terminated T/P was assessed by incubating 20 nM RT with 50 nM chain-terminated T/P in 50 mM Tris-HCl (pH 7.8), 60 mM KCl, and 10 mM $MgCl_2$. The reaction was initiated by the addition of either 100 μM pyrophosphate or 3 mM ATP, and TTP, dGTP, and dATP (10 μM each). Under these conditions, the extended primer rescue DNA polymerization product was seven nucleotides longer than the starting AZTMP-terminated primer. Aliquots were removed after various time intervals, quenched by the addition of an equal volume of sequencing gel loading buffer, and then analyzed by denaturing PAGE on 16% polyacrylamide−7 M urea gels. The 27-nucleotide rescue synthesis product was visualized and quantified by phosphorimaging.

Model Building. SYBYL (Tripos, St. Louis, MO) and O were used to prepare models of the complex of HIV-1 RT with AZTp4A. The starting atomic coordinates of HIV-1 RT were from the structure described by Huang et al. [PDB entry 1RTD (*21*)]. The side chain mutations T215Y, K70R, and M41L that are related to AZT resistance were manually modeled using conformations generally encountered in RT structures that carry such mutations. A 3′-OH group was added to the primer 3′-terminal 2′,3′-dideoxynucleotide of the input structure to emulate the natural primer. The dTTP at the active site of the ternary complex was converted to AZT-TP by adding an azido group at the 3′-position of dTTP in a conformation similar to that described in a related complex of RT with an AZTMP-terminated primer [PDB entry 1N5Y (*22*)]. The adenosine monophosphate component of AZTp4A was constructed manually on the basis of the structure of an adenosine triphosphate analogue [tenofovir diphosphate, PDB entry 1TO5 (*23*)]. It was initially placed in the active site by stacking the adenosine ring of the tetraphosphate on the tyrosine ring of Y215 and by placing the phosphate moiety proximal to the γ-phosphate of the AZTTP. The phosphate of adenosine monophosphate and the γ-phosphate of AZTTP were linked to construct the 5′−5′ tetraphosphate compound. The resulting AZTp4A was initially minimized using SYBYL with the surrounding protein constrained to adjust the ligand torsion angles and to bring the P−O bond distances to appropriate values (1.65

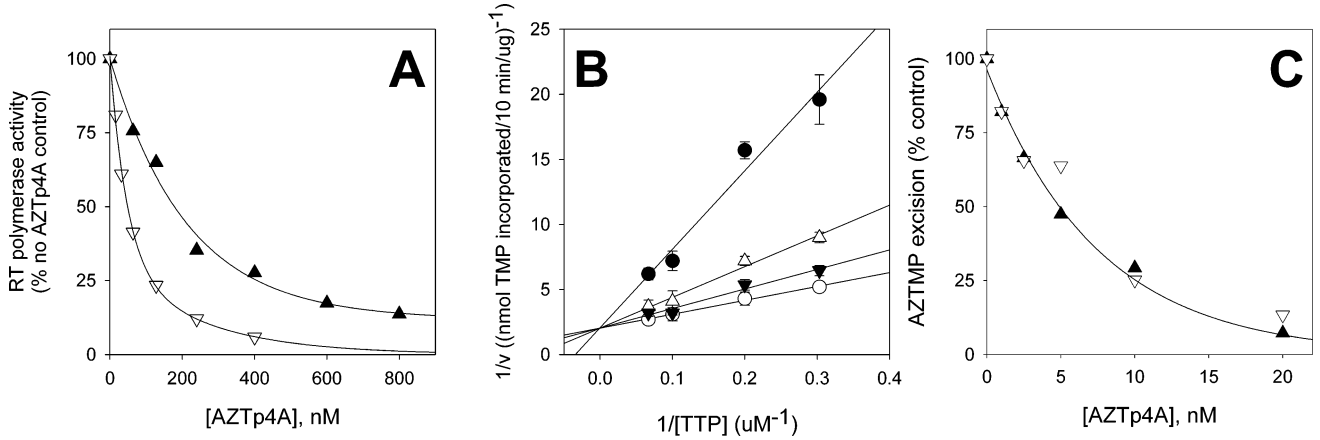

FIGURE 1: Inhibition of RT-catalyzed DNA synthesis and AZTMP excision by AZTp4A. (A) Dose dependence for inhibition of RNA-dependent DNA synthesis by AZTp4A catalyzed by wt RT (▲) and TAM-RT (▽), using poly(rA)-oligo(dT) as T/P and [^{3}H]TTP as substrate. (B) Double-reciprocal plots of TAM-RT-catalyzed RNA-dependent DNA synthesis using poly(rA)-oligo(dT) as T/P and [^{3}H]TTP as substrate in the presence of (○) no AZTp4A, (▼) 20 nM AZTp4A, (△) 100 nM AZTp4A, and (●) 250 nM AZTp4A. Data are means ± the standard deviation of triplicate determinations. (C) Dose dependence for inhibition of TAM-RT-catalyzed excision of 3′-terminal AZTMP by AZTp4A mediated by (▽) 150 μM PP_i or (▲) 3 mM ATP (in the presence of 0.01 unit of inorganic pyrophosphatase).

Å). Subsequently, close contacts with the protein were relieved by manual adjustments of torsion angles and local energy minimizations.

RESULTS

AZTp4A was a reasonable inhibitor of RT-catalyzed DNA polymerization measured with poly(rA)-oligo(dT) as the T/P (Figure 1A) and was approximately 7-fold more potent against TAM-RT ($IC_{50} = 38 \pm 2$ nM) than against the wt enzyme ($IC_{50} = 260 \pm 70$ nM). The mode of inhibition was competitive with respect to TTP substrate (Figure 1B). In contrast, AZTp4A exhibited little if any inhibition of TAM-RT polymerase reactions using dGTP and poly(rC)-oligo(dG) as T/P ($IC_{50} > 5$ μM; data not shown).

AZTp4A appeared to be an exceptionally potent inhibitor of both ATP-mediated and PP_i-mediated TAM-RT-catalyzed phosphorolytic excision when assessed in direct excision assays (Figure 1C; $IC_{50} \approx 5$ nM). AZTp4A was also evaluated in so-called "rescue" assays that measure the extent of RT-catalyzed DNA synthesis from a 3′-AZTMP-terminated primer in the presence of ATP or PP_i (*24*). In this assay, DNA synthesis can start only after removal of the chain-terminating 3′-AZTMP, which would be the rate-limiting step in the reaction. Thus, we expected that the inhibitory potency of AZTp4A would be reasonably similar in both direct and rescue excision assays. Surprisingly, the inhibitory potency of AZTp4A in the rescue assay was reduced more than 30-fold compared to that found in direct excision assays (data not shown).

An interesting observation in some preliminary direct excision assay experiments led us to suspect that AZTp4A might in fact act as a substrate for RT, like AZTTP. The primer used in these preliminary experiments was not completely terminated with AZTMP; thus, control samples showed both the 20-nucleotide AZTMP-terminated primer and small amounts (approximately 10%) of the 19-nucleotide unreacted starting primer. Control samples which contained this heterogeneous T/P substrate with RT and AZTp4A, but without ATP or PP_i, showed the disappearance of the 19-nucleotide nonterminated starting primer and a slight but reproducible increase in the amount of the 20-nucleotide terminated primer (data not shown). To confirm this observation, we directly examined the ability of AZTp4A to serve as a substrate for HIV-1 RT. Incubation of 2 μM AZTp4A, AZTTP, or TTP with RT and T/P resulted in extension of the primer by a single nucleotide (Figure 2A,B, lanes 4−9). Subsequent addition of dGTP and dATP extended the primer formed in the initial reaction with TTP by an additional seven nucleotides (Figure 2A,B, lanes 2 and 3). In contrast, no additional extension was seen with the primers formed in the initial incubations with either AZTp4A or AZTTP (Figure 2A,B, lanes 10−15). Furthermore, when initial reaction mixtures contained AZTp4A (or AZTTP), TTP, dATP, and dGTP (2 μM each), the predominant polymerization product was the 20-nucleotide single-nucleotide extended primer (Figure 2A,B, lanes 16−21). These data show that AZTp4A is a substrate for RT and that the single-nucleotide extended primer formed in the reaction with AZTp4A is unable to support additional extension, suggesting that AZTp4A is a chain terminator similar to AZTTP.

Panels C and D of Figure 2 show the concentration dependence of the substrate activity of AZTp4A and AZTTP under steady-state conditions with wt and TAM-RT, using heteropolymeric T/Ps. The apparent affinity of wt and TAM-RT for AZTTP is essentially similar (apparent $K_m \approx 0.5$ μM), whereas the affinity of wt RT for AZTp4A (apparent $K_m >$ 2 μM) is lower than that for AZTTP. In contrast, TAM-RT exhibits a 15-fold increased affinity for AZTp4A (apparent $K_m \approx 0.14$ μM) compared to wt RT. In addition, the affinity of TAM-RT for AZTp4A is 4-fold greater than that for AZTTP.

Pre-Steady-State Kinetic Analysis of AZTp4A and AZTTP as Substrates for HIV-1 RT. To better characterize the interaction of AZTp4A with HIV-1 RT, we carried out a series of pre-steady-state kinetic studies. Both pre-steady-state burst and single-turnover experiments were performed to compare the kinetics of incorporation of TTP, AZTTP, and AZTp4A.

Burst experiments used T/P in excess of RT. Under these conditions, a rapid initial rate of product formation due to incorporation of nucleotides by existing RT−T/P complexes is followed by a slower linear steady-state phase which

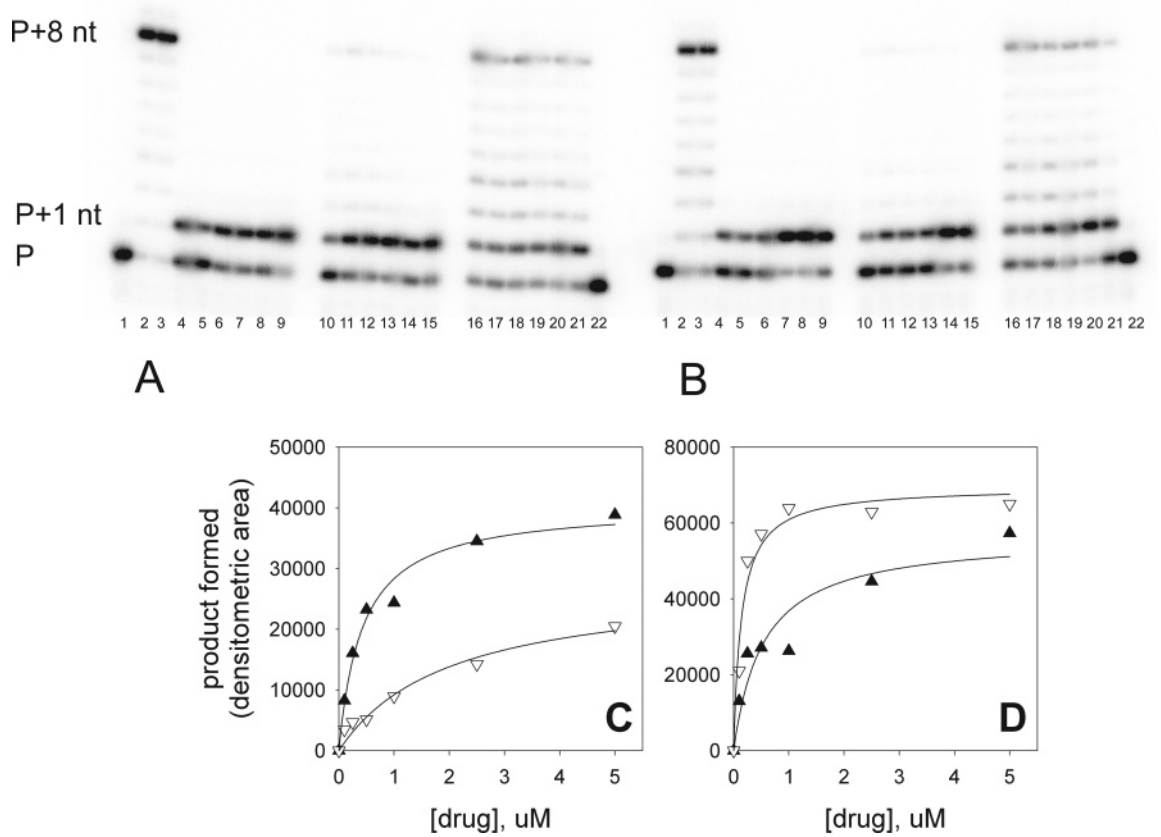

FIGURE 2: Primer extension catalyzed by RT in the absence and presence of AZTTP or AZTp4A. Reactions used 150 nM heteropolymeric 57/19 T/P and 40 nM RT as described in Experimental Procedures in the presence of (A) AZTp4A and TAM-RT or (B) AZTTP and TAM-RT: lanes 1 and 22, no RT control; lane 2, polymerization products formed after incubation for 20 min with TTP, dATP, and dGTP (2 μM each); lane 3, polymerization products formed after incubation for 20 min with 2 μM TTP followed by addition of dATP and dGTP (2 μM each) and additional incubation for 20 min; lanes 4−9, polymerization products formed after incubation for 20 min with 0.1, 0.25, 0.5, 1, 2.5, and 5 μM AZTp4A (A) or AZTTP (B), respectively; lanes 10−15, polymerization products formed after incubation for 20 min with 0.1, 0.25, 0.5, 1, 2.5, and 5 μM AZTp4A (A) or AZTTP (B), respectively, followed by addition of TTP, dATP, and dGTP (2 μM each) and additional incubation for 20 min; and lanes 16−21, polymerization products formed after incubation for 20 min with 0.1, 0.25, 0.5, 1, 2.5, and 5 μM AZTp4A (A) or AZTTP (B), respectively, in the presence of TTP, dATP, and dGTP (2 μM each). P is the 19-nucleotide starting primer, P+1nt the single-nucleotide extended primer, P+8nt the 27-nucleotide polymerization product formed in the presence of TTP, dATP, and dGTP. (C) P+1nt product formed by wt RT in the presence of varying concentrations of AZTp4A (▽) or AZTTP (▲). (D) P+1nt product formed by TAM-RT in the presence of varying concentrations of AZTp4A (▽) or AZTTP (▲).

defines the rate-limiting release of the single-nucleotide extended T/P. Under these conditions, the kinetics of incorporation of TTP, AZTTP, and AZTp4A were reasonably comparable (Figure 3 and Table 1).

The kinetics of incorporation of AZTTP and AZTp4A were also compared under single-turnover experiments using wt or TAM-RT in excess of T/P. Under these conditions, the entire prebound T/P is converted to the single-nucleotide extended primer product in a single kinetic step. Data from a typical experiment are shown in Figure 4A which illustrates the kinetics of single-nucleotide incorporation at varying AZTp4A concentrations catalyzed by TAM-RT. These experiments were used to define the maximum rate of incorporation (k_{pol}), the dissociation constant (K_d), and the catalytic efficiency of incorporation (k_{pol}/K_d) for AZTp4A and AZTTP for both wt and TAM-RT (Table 2). Although the maximum rate of incorporation (k_{pol}) of AZTp4A was essentially identical for wt and TAM-RT, the mutant enzyme exhibited a 6-fold increase in affinity (Table 2 and Figure 4B) and thus in catalytic efficiency for incorporation of AZTp4A. Interestingly, the catalytic efficiency of incorporation of AZTp4A by TAM-RT was nearly twice that for incorporation of AZTTP, suggesting that the tetraphosphate compound is a better chain-terminating substrate for TAM-RT than is AZTTP.

DISCUSSION

RT-catalyzed phosphorolytic excision of chain-terminating 3′-AZTMP is generally considered to be the major phenotypic mechanism for HIV resistance to AZT, and this phenotype may also contribute to resistance to other NRTIs as well. Both PP_i and ATP have been proposed as major substrates for the phosphorolytic excision reaction (*7*−*9*), although the substrate(s) used for NRTI excision during replication of AZT-resistant HIV is still unclear.

The product of PP_i-mediated excision of AZTMP is AZTTP. This newly formed AZTTP would presumably reside in the correct orientation to allow re-incorporation to the 3′-terminus of the primer. Such a scenario would result in a futile excision with no net benefit for HIV replication, unless AZTTP dissociation was rapid relative to the re-incorporation event. In this case, competition of TTP with the dissociated AZTTP could provide for continued reverse transcription following pyrophosphorolytic excision of the original 3′-terminal AZTMP.

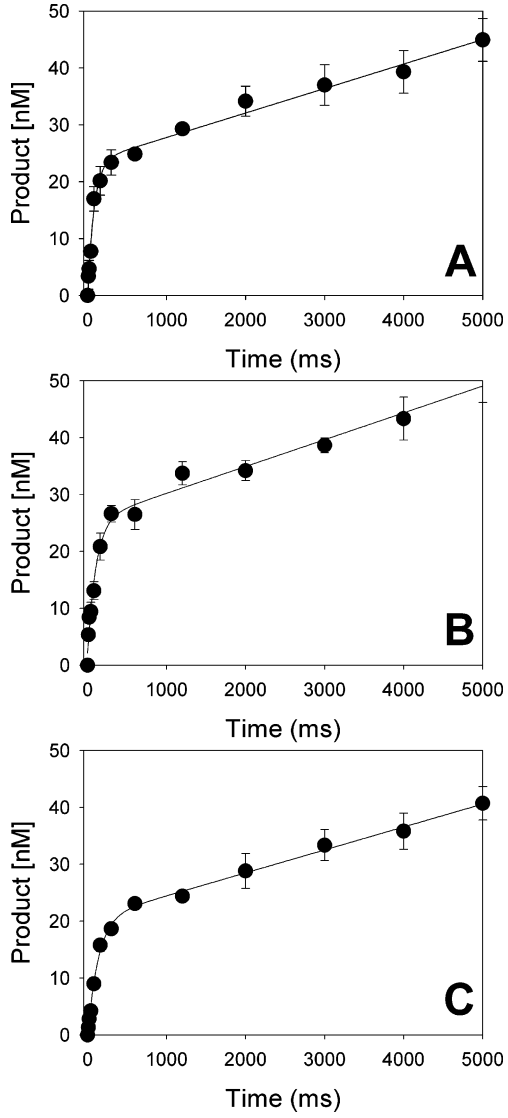

FIGURE 3: Pre-steady-state burst kinetics for incorporation of TTP (A), AZTTP (B), and AZTp4A (C) catalyzed by TAM-RT. RT (40 nM) was preincubated with 57/19 T/P (125 nM), and reactions were initiated by the addition of 40 μM nucleotide substrate and 10 mM $MgCl_2$. The reactions were quenched by the addition of EDTA to a final concentration of 0.2 M at the indicated time points. The data points are the means ± the standard deviation of three independent experiments. The lines are the best fit of the data to eq 1 described in Experimental Procedures. Kinetic constants from these experiments are listed in Table 1.

Table 1: Pre-Steady-State Kinetic Parameters for dTTP, AZTTP, and AZTp4A Incorporation with wt and TAM-RT

	wt RT		TAM-RT	
substrate	k_{obs} (s^{-1})	k_{ss} (s^{-1})	k_{obs} (s^{-1})	k_{ss} (s^{-1})
TTP	10.9 ± 0.6	4.7 ± 0.1	12.7 ± 1.7	4.2 ± 0.6
AZTTP	11.9 ± 2.5	3.0 ± 0.1	9.8 ± 2.0	4.7 ± 1.0
AZTp4A	8.6 ± 4.2	2.5 ± 0.7	7.3 ± 0.7	4.0 ± 0.8

The product of ATP-mediated excision is the dinucleoside 5′,5′-tetraphosphate compound, AZTp4A. This is a unique compound that likely arises only during ATP-mediated excision of chain-terminating 3′-AZTMP and which has no known biological properties. ATP might thus be a preferred excision substrate for TAM-RT since the reaction could lead to irreversible removal of 3′-terminal AZTMP as the novel product AZTp4A. While the cellular enzyme Ap4A hydrolase (asymmetrical dinucleoside tetraphosphatase) catalyzes the hydrolysis of AZTp4A resulting in the regeneration of AZTTP in many cell types (*25*), this reaction would occur away from the RT active site and thus the newly formed AZTTP would not be immediately available for reincorporation into the growing viral DNA. Victorova et al. (*15*) previously showed that HIV RT can use some bis(2′-deoxynucleoside)-5′,5′-tetraphosphates as substrates for DNA polymerization. However, these dinucleoside tetraphosphates are generally much less efficient substrates than the corresponding deoxynucleoside triphosphate. In contrast, we have found that AZTp4A is an excellent substrate for HIV RT

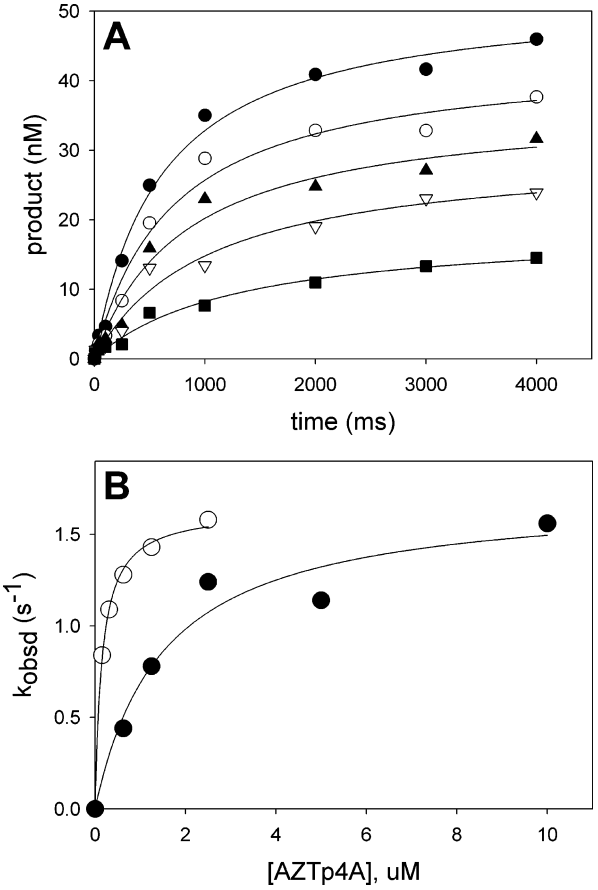

FIGURE 4: Kinetics for single-nucleotide incorporation of AZTp4A catalyzed by RT. Reactions used 150 nM RT and 50 nM 57/19 T/P as described in Experimental Procedures. (A) Rate of formation of the P+1nt product by TAM-RT in the presence of (■) 0.15, (▽) 0.31, (▲) 0.625, (O) 1.25, and (●) 2.5 μM AZTp4A. The lines are the best fit of the data to eq 2 described in Experimental Procedures. (B) Variation of k_{obs} with the concentration of AZTp4A in reactions catalyzed by wt RT (O) and TAM-RT (●). The lines are the best fit of the data to eq 3 described in Experimental Procedures. Kinetic constants from these experiments are listed in Table 2.

Table 2: Kinetic and Equilibrium Constants for Binding and Incorporation of AZTp4A and AZTTP by wt and TAM-RT

substrate	k_{pol} (s^{-1})	K_d (μM)	k_{pol}/K_d (μM^{-1} s^{-1})	catalytic efficiency ratio (TAM-RT/wt)
AZTp4A				
wt RT	2.1 ± 0.1	0.98 ± 0.08	2.1	
TAM-RT	1.9 ± 0.1	0.16 ± 0.01	11.9	5.7
AZTTP				
wt RT	10.0 ± 2.0	0.43 ± 0.06	23.2	
TAM-RT	7.5 ± 2.3	1.20 ± 0.1	6.2	0.3

with kinetic properties superior to those of either TTP or AZTTP, especially with TAM-RT (Table 2).

There are two possible extended primer products following use of AZTp4A as a substrate by RT, 3′-terminal AZTMP and 3′-terminal AMP. We propose that the product of the AZTp4A reaction is the 3′-AZTMP-terminated primer, for several reasons. First, our transient kinetic studies show that the mechanisms of the incorporation of AZTTP and AZTp4A are identical. Second, no additional polymerization is seen after addition of dNTPs to RT reaction mixtures following incubation with AZTp4A (Figure 2A), just as seen when AZTTP is incubated with RT, followed by addition of dNTPs (Figure 2B). RT is readily able to add 2′-deoxynucleotides to primers with a 3′-terminal ribonucleotide (*26*). If AMP was added to the primer terminus in the reaction with AZTp4A, then one might expect to see some evidence of the 27-nucleotide extended primer product following subsequent addition of dNTPs to the mixture. This extended primer is seen only in reactions that use TTP followed by addition of dATP and dGTP (Figure 2A,B, lanes 2 and 3). Third, the template base for the first nucleotide addition with the 57-nucleotide/19-nucleotide T/P used is adenine, which provides complementarity for thymidine nucleotides such as TTP, AZTTP, and the AZT component of AZTp4A. Addition of AMP from AZTp4A would constitute a mismatch or misincorporation. While RT is able to carry out misincorporation and mismatch extensions, these reactions are much less efficient than addition of the complementary nucleotide (*27*), and we believe that the chance of such misincorporation at the levels of AZTp4A used would be minimal. Furthermore, the asymmetric nature of the tetraphosphate comprising a 2′-deoxynucleoside component (AZT) and a ribonucleoside component (adenosine) should strongly favor the binding of the AZT end in the RT polymerase active site. The 2′-OH group of the adenosine end would be sterically excluded by Y115 that has been suggested to act as a "steric gate" to discriminate against ribonucleotides during RT-catalyzed DNA synthesis (*28*).

The ability of RT to use AZTp4A as a substrate also explains the rather substantial difference in apparent IC_{50} values (nearly 8-fold) for the inhibition by AZTp4A of DNA polymerization catalyzed by TAM-RT (38 ± 2 nM) compared to that for the inhibition of ATP-mediated AZTMP excision (ca. 5 nM) (Figure 1). The assay for phosphorolytic excision of chain-terminating AZTMP measures the extent of formation of a 19-nucleotide product from a 20-nucleotide AZTMP-terminated primer in a fixed time assay (as described in Experimental Procedures). AZTp4A is both an inhibitor of phosphorolytic excision and a substrate for RT. Thus, the presence of AZTp4A in excision reactions will lead to a substantially stronger inhibition of excision due to the use of the compound as a substrate, which will re-form the 20-nucleotide AZTMP-terminated starting primer. Subsequent measurement of the relative amounts of the 20-nucleotide starting primer and the 19-nucleotide excised primer will thus be inappropriately skewed toward the former.

The molecular basis for TAM-mediated enhancement of AZTMP excision is still unclear. Boyer et al. (*10*, *29*) proposed that TAMs increase the affinity of the mutant RT for ATP via aromatic stacking interactions between mutations such as Y/F215 and the adenine ring of ATP. However, others suggest that TAMs do not in fact increase the affinity of RT for ATP but rather act to properly position the ATP molecule in the RT active site to allow phosphorolytic excision to occur (*30*). It has also been proposed that enhanced excision of AZTMP may be due to tighter binding of the AZTMP-terminated P/T to TAM-RT which may facilitate pyrophosphorolysis by maintaining the AZTMP terminus in an appropriate position for excision (*31*). Our data show that the presence of TAMs in RT results in a substantial increase in the affinity of the enzyme for AZTp4A, which is supportive of the hypothesis of Boyer et al.

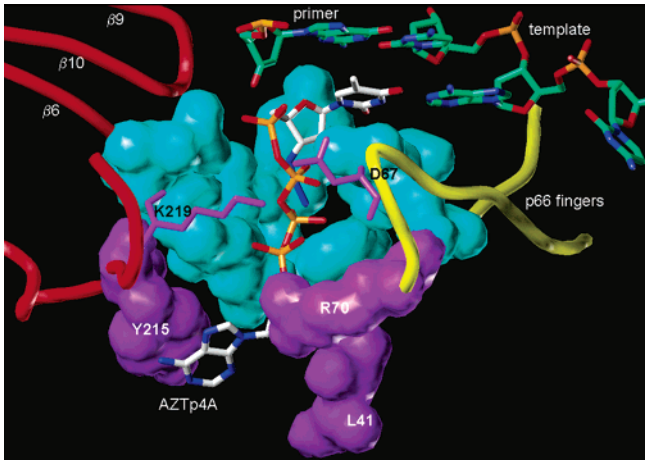

FIGURE 5: Molecular model for the interaction of AZTp4A with TAM-RT and double-stranded DNA T/P. The model was constructed as described in Experimental Procedures. The backbones of the palm and fingers subdomains are colored red and yellow, respectively; side chains of AZT resistance mutations are colored purple, and side chains of palm residues proximal to the modeled tetraphosphate are colored cyan.

We have developed a model for accommodating this enhanced binding by TAM-RT that may also explain the ability of AZTp4A to act as a chain-terminating substrate for HIV reverse transcriptase (Figure 5). The docked tetraphosphate has several interactions with RT both at the polymerase active site and at the proposed binding site of the ATP substrate for the excision reaction (*10*). In the polymerase active site, the AZT component of AZTp4A is bound in a manner similar to that of a bound dNTP substrate via base pairing interactions with the templating base and interactions with R72. The azido group interacts with the main chains of residues 113 and 114, plus the side chain of A114. This positions the $\alpha-\beta$ phosphodiester bond at the AZT end of the tetraphosphate in exactly the right position to allow nucleophilic attack by the 3′-OH group of the primer terminal nucleotide. The adenine base of AZTp4A stacks with the aromatic side chain of Y/F215 in a manner similar to that proposed for interaction of ATP with TAM-RT (*10*, *29*).

The model is consistent with our biochemical data in several ways. The affinity of TAM-RT for AZTp4A is 6-fold higher than that of wt RT. This increased affinity may result from stacking interactions of the adenine ring of AZTp4A with the tyrosine or phenylalanine at position 215 in TAM-RT. The equivalent residue in wt RT is threonine that would be unable to form any significant interactions with the adenine component of AZTp4A. The increased affinity of TAM-RT may also be due to interaction of the tetraphosphate

component of AZTp4A with other mutated residues common in the resistance of HIV to AZT such as D67N and K70R. The affinity of TAM-RT for AZTp4A is more than 7-fold greater than that of the same enzyme for AZTTP. This is again consistent with additional interactions of the adenine ring of AZTp4A with TAMs, interactions that are absent in binding of AZTTP.

It is important to note that our model not only describes the binding of RT to an exogenously added AZTp4A but also would represent the complex of RT with a newly formed AZTp4A molecule arising from ATP-mediated phosphorolytic excision of terminating AZTMP. Our model therefore suggests that the newly excised AZTMP, as AZTp4A, has the potential of being immediately re-incorporated by RT, analogous to that of the AZTTP formed during pyrophosphorolytic excision. Release of the excision products formed during both pyrophosphorolysis and ATP-mediated phosphorolysis is thus likely to constitute the critical step for the continued synthesis of viral DNA. The substantially increased affinity of TAM-RT for AZTp4A compared to that of the wt enzyme, when contrasted with the somewhat reduced affinity of the mutant enzyme for AZTTP, suggests that ATP may not be an optimal excision substrate during replication of AZT-resistant HIV. Furthermore, even if AZTp4A is released before re-incorporation of AZTMP can occur, the cellular enzyme Ap4A hydrolase can convert AZTp4A to AZTTP (*23*) that can then be incorporated into the viral DNA. In light of these observations, more detailed mechanistic studies with other potential pyrophosphate donors such as GDP and ADP, shown to produce excision products in cell extracts (*32*), may be warranted.

ACKNOWLEDGMENT

We thank Sean McBurney and Dr. Dominique Arion for useful input in the early stages of this work.

REFERENCES

1. Lightfoote, M. M., Coligan, J. E., Folks, T. M., Fauci, A. S., Martin, M. A., and Venkatesan, S. (1986) Structural characterization of reverse transcriptase and endonuclease polypeptides of the acquired immunodeficiency syndrome retrovirus, *J. Virol. 60*, 771−775.
2. Baltimore, D. (1970) RNA-dependent DNA polymerase in virions of RNA tumour viruses, *Nature 226*, 1209−1211.
3. Goody, R. S., Müller, B., and Restle, T. (1991) Factors contributing to the inhibition of HIV reverse transcriptase by chain-terminating nucleotides in vitro and in vivo, *FEBS Lett. 291*, 1−5.
4. Schinazi, R. F., Larder, B. A., and Mellors, J. M. (2000) Mutations in retroviral genes associated with drug resistance: 2000−2001. Update, *Int. Antiviral News 8*, 65−91.
5. Sluis-Cremer, N., Arion, D., and Parniak, M. A. (2000) Molecular mechanisms of HIV-1 resistance to nucleoside reverse transcriptase inhibitors (NRTIs), *Cell. Mol. Life Sci. 57*, 1408−1422.
6. Selmi, B., Deval, J., Boretto, J., and Canard, B. (2003) Nucleotide analogue binding, catalysis and primer unblocking in the mechanisms of HIV-1 reverse transcriptase-mediated resistance to nucleoside analogues, *Antiviral Ther. 8*, 143−154.
7. Arion, D., Kaushik, N., McCormick, S., Borkow, G., and Parniak, M. A. (1998) Phenotypic mechanism of HIV-1 resistance to 3′-azido-3′-deoxythymidine (AZT): Increased polymerization processivity and enhanced sensitivity to pyrophosphate of the mutant viral reverse transcriptase, *Biochemistry 37*, 15908−15917.
8. Meyer, P. R., Matsuura, S. E., So, A. G., and Scott, W. A. (1998) Unblocking of chain-terminated primer by HIV-1 reverse transcriptase through a nucleotide-dependent mechanism, *Proc. Natl. Acad. Sci. U.S.A. 95*, 13471−13476.
9. Meyer, P. R., Matsuura, S. E., Mian, A. M., So, A. G., and Scott, W. A. (1999) A mechanism of AZT resistance: An increase in nucleotide-dependent primer unblocking by mutant HIV-1 reverse transcriptase, *Mol. Cell 4*, 35−43.
10. Boyer, P. L., Sarafianos, S. G., Arnold, E., and Hughes, S. H. (2001) Selective excision of AZTMP by drug-resistant human immunodeficiency virus reverse transcriptase, *J. Virol. 75*, 4832−4842.
11. Larder, B. A., and Kemp, S. D. (1989) Multiple mutations in HIV-1 reverse transcriptase confer high-level resistance to zidovudine (AZT), *Science 246*, 1155−1158.
12. Larder, B. A., Kellam, P., and Kemp, S. D. (1991) Zidovudine resistance predicted by direct detection of mutations in DNA from HIV-infected lymphocytes, *AIDS 5*, 137−144.
13. Larder, B. A. (1994) Interactions between drug resistance mutations in human immunodeficiency virus type 1 reverse transcriptase, *J. Gen. Virol. 75*, 951−957.
14. Kellam, P., Boucher, C. A. B., and Larder, B. (1992) Fifth mutation in human immunodeficiency virus type 1 reverse transcriptase contributes to the development of high-level resistance to zidovudine, *Proc. Natl. Acad. Sci. U.S.A. 89*, 1934−1938.
15. Victorova, L., Sosunov, V., Skoblov, A., Shipytsin, A., and Krayevsky, A. (1999) New substrates of DNA polymerases, *FEBS Lett. 453*, 6−10.
16. Fletcher, R. S., Holleschak, G., Nagy, E., Arion, D., Borkow, G., Gu, Z., Wainberg, M. A., and Parniak, M. A. (1996) Single-step purification of recombinant wild-type and mutant HIV-1 reverse transcriptase, *Protein Expression Purif. 7*, 27−32.
17. Hanna, G. J., Johnson, V. A., Kuritzkes, D. R., Richman, D. D., Leigh Brown, A. J., Savara, A. V., Hazelwood, J. D., and D'Aquila, R. T. (2000) Patterns of resistance mutations selected by treatment of human immunodeficiency virus type 1 infection with zidovudine, didanosine, and nevirapine, *J. Infect. Dis. 181*, 904−911.
18. Kati, W. M., Johnson, K. A., Jerva, L. F., and Anderson, K. S. (1992) Mechanism and fidelity of HIV reverse transcriptase, *J. Biol. Chem. 267*, 25988−25997.
19. Meyer, P. R., Smith, A. J., Matsuura, S. E., and Scott, W. A. (2004) Effects of primer-template sequence on ATP-dependent removal of chain-terminating nucleotide analogues by HIV-1 reverse transcriptase, *J. Biol. Chem. 279*, 45389−45398.
20. Kerr, S. G., and Anderson, K. S. (1997) Pre-steady-state kinetic characterization of wild type and 3′-azido-3′-deoxythymidine (AZT) resistant human immunodeficiency virus type 1 reverse transcriptase: Implication of RNA directed DNA polymerization in the mechanism of AZT resistance, *Biochemistry 36*, 14064−14070.
21. Huang, H., Chopra, R., Verdine, G. L., and Harrison, S. C. (1998) Structure of a covalently trapped catalytic complex of HIV-1 reverse transcriptase: Implications for drug resistance, *Science 282*, 1669−1675.
22. Sarafianos, S. G., Clark, A. D., Das, K., Tuske, S., Birktoft, J. J., Ilankumaran, P., Ramesha, A. R., Sayer, J. M., Jerina, D. M., Boyer, P. L., Hughes, S. H., and Arnold, E. (2002) Structures of HIV-1 reverse transcriptase with pre- and post-translocation AZTMP-terminated DNA, *EMBO J. 21*, 6614−6624.
23. Tuske, S., Sarafianos, S. G., Clark, A. D., Ding, J., Naeger, L. K., White, K. L., Miller, M. D., Gibbs, C. S., Boyer, P. L., Clark, P., Wang, G., Gaffney, B. L., Jones, R. A., Jerina, D. M., Hughes, S. H., and Arnold, E. (2004) Structures of HIV-1 RT-DNA complexes before and after incorporation of the anti-AIDS drug tenofovir, *Nat. Struct. Mol. Biol. 11*, 469−474.
24. Arion, D., Sluis-Cremer, N., and Parniak, M. A. (2000) Mechanism by which phosphonoformic acid resistance mutations restore 3′-azido-3′-deoxythymidine (AZT) sensitivity to AZT-resistant HIV-1 reverse transcriptase, *J. Biol. Chem. 275*, 9251−9255.
25. Pitcher, W. H., III, Kirby, T. W., DeRose, E. F., and London, R. E. (2003) Metabolic transformation of AZTp4A by Ap4A hydrolase regenerates AZT triphosphate, *Antiviral Res. 58*, 227−233.
26. Thrall, S. H., Krebs, R., Wohrl, B. M., Cellai, L., Goody, R. S., and Restle, T. (1998) Pre-steady-state kinetic characterization of RNA-primed initiation of transcription by HIV-1 reverse transcriptase and analysis of the transition to a processive DNA-primed polymerization mode, *Biochemistry 37*, 13349−13358.
27. Kerr, S. G., and Anderson, K. S. (1997) RNA dependent DNA replication fidelity of HIV-1 reverse transcriptase: Evidence of discrimination between DNA and RNA substrates, *Biochemistry 36*, 14056−14063.

28. Gao, G., Orlova, M., Georgiadis, M. M., Hendrickson, W. A., and Goff, S. P. (1997) Conferring RNA polymerase activity to a DNA polymerase: A single residue in reverse transcriptase controls substrate selection, *Proc. Natl. Acad. Sci. U.S.A. 94*, 407−411.
29. Sarafianos, S. G., Hughes, S. H., and Arnold, E. (2004) Designing anti-AIDS drugs targeting the major mechanism of HIV-1 RT resistance to nucleoside analog drugs, *Int. J. Biochem. Cell Biol. 36*, 1706−1715.
30. Ray, A. S., Murakami, E., Basavapathruni, A., Vaccaro, J. A., Ulrich, D., Chu, C. K., Schinazi, R. F., and Anderson, K. S. (2003) Probing the molecular mechanisms of AZT drug resistance mediated by HIV-1 reverse transcriptase using a transient kinetic analysis, *Biochemistry 42*, 8831−8841.
31. Canard, B., Sarfati, S. R., and Richardson, C. C. (1998) Enhanced binding of azidothymidine-resistant human immunodeficiency virus 1 reverse transcriptase to the 3′-azido-3′-deoxythymidine 5′-monophosphate-terminated primer, *J. Biol. Chem. 273*, 14596−14604.
32. Smith, A. J., Meyer, P. R., Asthana, D., Ashman, M. R., and Scott, W. A. (2005) Intracellular substrates for the primer-unblocking reaction by human immunodeficiency virus type 1 reverse transcriptase: Detection and quantitation in extracts from quiescent- and activated-lymphocyte subpopulation, *Antimicrob. Agents Chemother. 49*, 1761−1769.

BI061364S